Modelling mixotrophic functional diversity and implications for ecosystem function

SUZANA GONÇALVES LELES[1,2*], LUCA POLIMENE[1], JORN BRUGGEMAN[1], JEREMY BLACKFORD[1], STEFANO CIAVATTA[1,3], ADITEE MITRA[2], AND KEVIN JOHN FLYNN[2]

[1]Plymouth Marine Laboratory, Prospect Place, Plymouth, PL1 3DH, UK
[2]Swansea University, Singleton Park, Swansea SA2 8PP, UK.
[3]National Centre for Earth Observation, Plymouth Marine Laboratory, Prospect Place, The Hoe, Plymouth PL1 3DH, UK

*correspondence to: sul@pml.ac.uk

Abstract

Mixotrophy is widespread among protist plankton displaying diverse functional forms within a wide range of sizes. However, little is known about the niches of different mixotrophs and how they affect nutrient cycling and trophodynamics in marine ecosystems. Here we built a plankton food web model incorporating mixotrophic functional diversity. A distinction was made between mixotrophs with innate capacity for photosynthesis (constitutive mixotrophs, CMs) and those which acquire phototrophy from their prey (non-constitutive mixotrophs, NCMs). We present simulations of ecosystems limited by different light and nutrient regimes. Our simulations show that strict autotrophic and heterotrophic competitors increased in relative importance in the transition from nutrient to light limitation, consistent with observed oceanic biomass ratios. Among CMs, cells < 20 µm dominate in nutrient poor conditions while larger cells dominate in light-limited environments. The specificity of the prey from which NCMs acquire their phototrophic potential affects their success, with forms able to exploit diverse prey dominating under nutrient limitation. Overall, mixotrophy decreases regeneration of inorganics and boosts the trophic transfer efficiency of carbon. Our results show that mixotrophic functional diversity has the potential to radically change our understanding of the ecosystem functioning in the lower trophic levels of food webs.

keywords: mixotrophy, acquired phototrophy, marine plankton, functional diversity, size, ecosystem model, ERSEM

Introduction

Food webs comprise complex arrays of interactions between resources and consumers (Worm *et al*., 2002; Araújo *et al*., 2011). Despite the recognised importance of predation and competition in defining the ecological niches of different functional taxa (Hunter and Price 1992; Cloern and Dufford, 2005), the overall structure and dynamics of food webs are also greatly affected by additional factors, such as intraguild predation and omnivory (Polis *et al*., 1989; Williams and Martinez, 2000; Johnson *et al*., 2010; Granados *et al*., 2017). Mixotrophy, defined here as the combination of phototrophy and phagotrophy in a single organism (Table I), is another 'twist' that can shift our understanding of ecosystem dynamics from terrestrial to aquatic environments (Tittel *et al*., 2003; Selosse *et al*., 2017).

Mixotrophy among protist plankton is near ubiquitous in the sunlit ocean and has been observed among all dominant protist classes (from the largest to the smallest), with diatoms being the only exception (Zubkov and Tarran, 2008; Flynn *et al*., 2013; Biard *et al*., 2016; Stoecker *et al*., 2017). Accordingly, protist plankton have been recently regrouped to better represent their physiological functionality in terms of energy and nutrient acquisition (Mitra *et al*., 2016). A critical feature of this functionality is that mixotrophs can be divided amongst organisms with a constitutive ability to photosynthesise (the constitutive mixotrophs, CMs) and those that do not possess the innate ability to fix carbon dioxide but acquire this ability from their prey (the non-constitutive mixotrophs, NCMs) (Table I) (Mitra *et al*., 2016). NCMs are further divided into generalist forms (GNCMs) that can exploit plastids acquired from diverse phototrophic prey, and specialist forms (SNCMs) that must acquire the phototrophic machinery from specific prey (Table I) (Stoecker *et al*., 2009; Johnson *et al*., 2011; Mitra *et al*., 2016). Thus, while conceptual food webs traditionally divide the plankton into phytoplankton or zooplankton, this dichotomy comprehensively misrepresents reality, with most protist 'phytoplankton' capable of grazing, and ca. half of the 'microzooplankton' capable of photosynthesis (Flynn *et al*., 2013; Stoecker *et al*., 2017).

There is a need to understand how mixotrophy, in its different forms, may change our understanding and simulations of food web dynamics and biogeochemical cycling in the oceans. For instance, CMs have been hypothesized to 'farm' bacteria in oligotrophic waters; while CMs feed on bacteria to acquire essential nutrients, they also release dissolved organic matter (DOM) which supports bacterial growth (Mitra *et al*., 2014). Mixotrophs, compared to their heterotrophic competitors, can retain more nutrients from their prey as they can use them along with the organic carbon obtained through photosynthesis. An implication of this is, if mixotrophs outcompete strict heterotrophs in oligotrophic regions, then nutrient limitation of pure autotrophs (including cyanobacteria) may become more severe (Fischer *et al*., 2016). Furthermore, NCMs have the clear potential to achieve higher gross growth efficiencies through acquired phototrophy, potentially

increasing the transfer of carbon biomass to higher trophic levels, particularly in low chlorophyll waters (Stoecker *et al*., 2009). Taken together these studies suggest that mixotrophy has the potential to enhance both the production of large size, fast sinking particles (e.g. faecal pellets) by mesozooplankton, which may feed on mixotrophs, and the bacterial production of recalcitrant material (Jiao *et al*., 2010; Polimene *et al*., 2017) which may be stimulated by the enhanced production of dissolved organic carbon (DOC) (Mitra *et al*., 2014). Both the production of particles and recalcitrant DOC are key fluxes for the global carbon cycle contributing to the ocean carbon sequestration (Legendre *et al*., 2015).

So far, few studies have investigated the relevance of functional diversity within the mixotrophs on food web functioning and ecosystem properties (Flynn and Mitra, 2009; Mitra *et al*., 2016; Ghyoot *et al*., 2017). Understanding the ecological niches of mixotrophs and their strict auto- and hetero- trophic competitors helps to identify when and where different mixotrophs are major components of plankton communities and, thus, potentially affect ecosystem properties (Fischer *et al*., 2016; Leles *et al*., 2017). Mixotrophic functional diversity is a topic of particular importance in the context of climatic and anthropogenic changes on the oceans. Consider plankton communities in two contrasting marine ecosystems, oligotrophic seas and eutrophic coastal systems, characterised by nutrient and light limitation, respectively. Global warming is expected to increase ocean stratification in the former, potentially expanding the area occupied by low productive seas (Polovina *et al*., 2008; Behrenfeld *et al*., 2016). In turn, the increased runoff of nutrients and organic matter in coastal waters usually promotes unbalanced (and high) nitrogen to phosphorus ratios (Burkholder *et al*., 2008; Gomes *et al*., 2014). In both cases, mixotrophy has been shown to be a successful strategy (Burkholder *et al*., 2008; Zubkov and Tarran, 2008; Wilken *et al*., 2013; Gomes *et al*., 2014). Thus, acknowledging the role of mixotrophs can be key to predict the dynamics of plankton communities in a changing ocean.

While there is increasing awareness that mixotrophy is a key trait shaping biological communities, quantifying its physiological and ecological relevance is challenging (Selosse *et al*., 2017). This lack of knowledge is mainly due to the difficulty to accurately characterise the abundance and distributions of mixotrophs in the field (Anderson *et al*., 2017). Modelling studies provide a suitable platform to investigate the effects of mixotrophs on ecosystem function by using a hypothesis testing approach. Although several studies have simulated mixotrophy (Thingstad *et al*., 1996; Stickney *et al*., 2000; Flynn and Mitra, 2009, Flynn and Hansen, 2013; Våge *et al*., 2013; Mitra *et al*., 2014; Mitra *et al*., 2016; Moeller *et al*., 2016), few have accounted for mixotrophic functional diversity and their impact on ecosystem dynamics (Ghyoot *et al*., 2017). In addition, the structure of the mixotroph model is very important; mixotrophy does not simply reflect the additive

interaction between phototrophy and phagotrophy and the description of metabolic switching from one strategy to the other is important to correctly simulate metabolic rates (Mitra and Flynn, 2010).

Here we combined, for the first time, models of diverse types of mixotrophs across different size classes with submodels of plankton as described in the European Regional Seas Ecosystem Model (ERSEM; Baretta-Bekker *et al*., 1995; Butenschön *et al*., 2016). The impact of mixotrophic functional diversity on key biogeochemical fluxes and plankton trophodynamics was assessed by contrasting our model with a 'non-mixotrophic' plankton food web model. Since mixotrophy is expected to dominate in mature ecosystems in which resources are limiting, we simulated nutrient or light limitation scenarios, akin to conditions representative of oligotrophic seas and eutrophic coastal systems, respectively. Our theoretical framework allows the investigation of the relative importance of constitutive and non-constitutive mixotrophs (CMs and NCMs) and of their strict autotrophic and heterotrophic competitors.

The Model

The food webs

We compared two plankton food webs (named here as 'non-mixotrophic' and 'mixotrophic' food webs) that differ only in the inclusion of mixotrophic functional types (Fig. 1). The community structure of the non-mixotrophic food web was defined following the conceptual framework of ERSEM (Baretta-Bekker *et al*., 1995; Butenschön *et al*., 2016). This non-mixotrophic food web comprised eight functional groups that differ mainly in size and trophic strategy (Fig. 1): four phototrophs (picophytoplankton, nanoflagellates, microflagellates, and diatoms), three predators (nanoflagellates, microzooplankton, and mesozooplankton), and one decomposer (heterotrophic bacteria). Here, heterotrophic nanoflagellates feed on pico- and nano- sized prey, microzooplankton feed on pico-, nano-, and micro-sized prey, and mesozooplankton feed on nano- and micro- sized prey (Fig. 1). Intraguild predation was allowed among all predators.

In the mixotrophic food web, nanoflagellates and microflagellates (previously perceived as strict autotrophs) were allowed to feed on diverse prey items, as supported by evidence from the literature (Zubkov and Tarran, 2008; Jeong *et al*., 2010; Hansen, 2011; Unrein *et al*., 2014). These constitutive mixotrophs are called hereafter as CM-nano and CM-micro, respectively (Table I). They can access the same prey as their heterotrophic competitors of same size (heterotrophic nanoflagellates and microzooplankton, respectively; Fig. 1 and Table S1). In turn, the microzooplankton group was divided into strict heterotrophic species and NCMs; previous estimates suggest that 40–60% of total microzooplankton can acquire phototrophic potential (Dolan and Pérez, 2000; Leles *et al*., 2017). They share the same prey items and were assumed not to feed on each other (Fig. 1). Our conceptual framework accounted for GNCMs, such as oligotrich ciliates,

which have lower control over the acquired phototrophic machinery but can obtain it from diverse prey items, and SNCMs, such as *Mesodinium rubrum*, which have higher control over the acquired phototrophic machinery but rely on specific prey (Mitra *et al*., 2016). SNCMs must obtain the phototrophic potential by feeding on CM-nano, while GNCMs can also obtain it feeding on CM-micro (Stoecker *et al*., 1988-1989; Gustafson *et al*., 2000; Johnson *et al*., 2007; McManus *et al*., 2012). Intraguild predation was allowed within each mixotrophic functional type (Fig. 1, Table S1).

The model resolves the major chemical elements in the ocean, i.e. carbon, nitrogen, phosphorus, and silicate, both in organic and inorganic forms, accounting for variable stoichiometry within plankton groups (except for within mesozooplankton where C:N:P was held constant). Protist functional groups were described by a general plankton model that develops from the previous work by Flynn and Mitra (2009) and Mitra *et al*. (2016). Nutrient pools and the bacteria and mesozooplankton submodels correspond to those of ERSEM (Butenschön *et al*., 2016) and are described further below. Overall, plankton growth dynamics result from the balance of gains through uptake of nutrients and assimilation into organic compounds and losses through respiration, excretion (non-assimilated material) and/or release of excess of nutrients (linked to stoichiometric regulation), predation, and non-predatory mortality (e.g. viral lysis). All state variables have units of element concentration (e.g. mg C m^{-3}). Model equations and parameter values can be found in the supplementary material (Tables S2–S5). Our model was implemented in the open source Fortran-based Framework for Aquatic Biogeochemical Models (FABM) (Bruggeman and Bolding, 2014), an open platform (available at http://fabm.net) through which different models or submodels may be coupled in a single framework.

Nutrients, dissolved, and particulate organic matter

Nutrient pools were divided between inorganics (nitrate, ammonium, phosphate, silicate, and dissolved inorganic carbon), dissolved organic matter (DOM), and detrital particulate organic matter (POM). DOM was divided between labile and semi-labile assuming that the former is rapidly consumed by bacteria and that the latter is more resistant to microbial degradation (Hansell, 2013). Detrital POM was divided in three size-classes assuming that mesozooplankton can scavenge only on the medium size fraction. The chemical and the biological components of the food web model interact through the uptake of inorganics and the formation and recycling of organics, as described below for protists, bacteria, and mesozooplankton.

Protists

The general protist model has the potential to simulate any protist from strict autotrophs to strict heterotrophs, including CMs and NCMs (see Supplementary Methods). The uptake of inorganics, photoacclimation, prey ingestion, and acquired phototrophy can be enabled/disabled accordingly. Here, we describe the main modifications and/or additions applied to the protist model

with respect to Flynn and Mitra (2009); equations can be found in the Supplementary Material. We developed the model in four main aspects:

i) We implemented the uptake of silicon to simulate diatoms following Flynn (2005). The representation of diatoms differs from that of other phototrophic protists due to their physiological requirement for silicon to build their frustules. In turn, silicon uptake differs fundamentally from that of nitrogen and phosphorus because the external nutrient concentration, instead of the internal (nutrient quota) concentration, ultimately affects growth; consequently, quota models are inappropriate for silicon dynamics (Flynn and Martin-Jézéquel, 2000).

ii) We implemented the allometric description of predation as described by Flynn and Mitra (2016). This formulation simulates the kinetics of prey capture and ingestion relating prey abundance and encounter rates to a prey-selection function controlled by satiation. In our model, prey selection is controlled by the total prey size spectrum accessible by the predator and its optimal prey size; capture is then minimum on both extremes of the prey size spectrum increasing linearly towards the optimal prey size (Flynn, 2018). This approach is very similar to the Gaussian predation kernel, but our formulation has the additional benefit of being defined directly by the observable lower and upper prey size limits.

iii) Acquired phototrophy was modified so that kleptochloroplasts are not digested but lost over time at a constant rate (Flynn and Hansen, 2013).

iv) All model equations were modified so that state variables were expressed in units of element quantity per water volume to allow model coupling with ERSEM submodels.

In our food webs, strict autotrophs can photoacclimate through the synthesis of chlorophyll, take up ammonium, nitrate, and phosphorus (plus silicon if diatoms), release labile DOC during photosynthesis, release labile DOM due to non-predatory mortality, and release dissolved inorganic carbon (DIC) and excess of inorganic nutrients (ammonium and phosphate) as part of respiration and stoichiometric regulation, respectively. Parameter values controlling light harvesting and nutrient uptake defined the differences between strict autotrophs in the model. In addition, CMs can engage in phagotrophy, re-assimilate inorganic nutrients released by breaking down their prey, and excrete the non-assimilated material as labile DOM. CMs must acquire a critical proportion of growth through photosynthesis and phagotrophy can be down-regulated if enough carbon is provided through phototrophy (Hansen, 2011). The model assumed that the internal re-assimilation of nutrients depends on the stoichiometric status of the mixotroph (N or P stress). We also assumed that CMs have lower maximum growth rates (μ_{max}) compared to their heterotrophic competitors (Fischer *et al*., 2016). On top of the differences related to light harvesting and nutrient uptake, CM-nano and CM-micro differ in their predation impact, with the former selecting pico-sized prey and having a narrower prey size spectrum, while the later selects for nano-sized prey (Table S1).

Strict heterotrophs assimilate organics through predation and release labile DOM due to non-predatory mortality, DIC through respiration, and non-assimilated material as labile DOM. The same processes were applied to NCMs, but these can fix inorganic carbon through acquired phototrophy (but do not photoacclimate), take up external inorganic nutrients (only SNCMs), and re-assimilate inorganic nutrients internally. Heterotrophic nanoflagellates select pico-size prey and have a narrower prey size spectrum while microzooplankton and NCMs select for nano-sized prey. NCMs were assumed to have the same μ_{max} as their heterotrophic counterparts, to select autotrophic prey, and to be positively selected by mesozooplankton compared to strict heterotrophic microzooplankton (Dolan and Pérez, 2000; Broglio *et al*., 2004; Figueiredo *et al*., 2007; Schoener and McManus, 2017). Among NCMs, GNCMs retain chloroplasts from their prey while SNCMs can also retain other cellular components and largely rely on photosynthesis to obtain carbon; thus, SNCMs were assumed to rely on photosynthesis for a critical proportion of growth while GNCMs were not (Stoecker *et al*., 2009). In addition, SNCMs have better control over the acquired phototrophic machinery compared to GNCMs (Stoecker *et al*., 2009); thus, our model assumes lower loss rate of kleptochloroplasts for the former.

Decomposers

Bacteria were assumed to consume all forms of particulate and dissolved organic matter and to take up or release inorganic nutrients depending on the quality (i.e. N and P relative content) of the organic matter. Bacteria thus compete with phytoplankton for inorganic nutrients when organic substrates are nutrient depleted. Bacteria were assumed to release any carbon in excess to their physiological requirement (which is regulated by an 'optimal' cellular carbon to nutrient ratio) as semi-labile DOC. Recalcitrant DOC was also produced by the release of capsular material (Stoderegger and Herndl, 1998) which was assumed to be a fixed proportion of the carbon uptake. Overall these two fluxes imply that bacteria (especially when feeding on carbon-rich substrates) change the quality of DOM, increasing the proportion of recalcitrant DOC with respect to the labile forms. This mechanism is consistent with the microbial carbon pump concept (Jiao *et al*., 2010; Polimene *et al*., 2017).

Mesozooplankton

The mesozooplankton model assumes a fixed internal nutrient to carbon ratio and the ability to scavenge on particulate organic matter. We modified the predation function from ERSEM to be consistent with that used in the protist model but through a simpler description; clearance rate is prey specific and was defined by the biomass of prey multiplied by the slope of the relationship between the abundance of prey and capture (Flynn and Mitra, 2016). Prey preference was based on size and depends on functional type. Mesozooplankton release excess nutrients as ammonium and

phosphate and contribute both to the pool of dissolved and particulates through mortality and excretion (e.g. faecal pellets).

Model set-up

The food webs were simulated through chemostat-like modelling experiments. The model assumes plankton biomass and nutrients to vary over time within a homogeneous "box" that receives a constant input of inorganic nutrients (nitrate, phosphate, silicate) through a constant dilution rate. The same dilution rate also washes out residual nutrients and other dissolved and particulate organics (including plankton) and inorganics from the system. This construct is thus akin to a mixed layer environment which is subjected to an input of nutrients from a steady deeper layer, i.e. which does not accumulate properties over time. We assumed a fixed depth of 10 m, 12:12 hours light-dark cycle, a constant temperature of 10ºC, and a constant dilution rate of 0.01 day^{-1}. The photosynthetically active radiation (PAR) was computed from the shortwave radiation in the surface (I_{surf}), which was assumed to be constant through the period of the simulation, and an attenuation coefficient dependent on the concentration of plankton and particulate organic matter. The concentration of inorganics (e.g. dissolved inorganic nitrogen – DIN) entering the system (akin to concentrations below the mixed layer) was constant throughout a given simulation.

We simulated two different scenarios: low light-high nutrient (I_{surf} = 50 W m^{-2} or 228 µmol photon m^{-2} s^{-1}; DIN = 20 µM nitrate) and high light-low nutrient (I_{surf} = 250 W m^{-2} or 1,140 µmol photon m^{-2} s^{-1}; DIN = 4 µM nitrate). These irradiance and nutrient concentrations were chosen to induce light limitation or nutrient limitation among phototrophs. Light limitation was assessed through the relative rate of photosynthesis (i.e. the ratio between the actual photosynthesis rate and the maximum photosynthesis rate) while nutrient limitation was assessed through the normalised nutrient to carbon quotas. We assumed an input 16:1 mole ratio of dissolved inorganic nitrogen (DIN; nitrate) to phosphorus, and a 1:1 mole ratio of DIN to silicon in all simulations.

Models output are presented herein through the average of the last year of simulation. Dynamic plots can be found in the supplementary material (Figs. S2–S6). We compared: i) the total ammonium regeneration, ii) the trophic transfer efficiency, and iii) the total production of labile DOC between the non-mixotrophic and the mixotrophic food webs. These metrics were chosen to test the hypotheses that mixotrophy decreases the overall regeneration of inorganics, increases the transfer of biomass to higher trophic levels promoting the accumulation of biomass in larger size-classes and increases DOC production. The ratio between the total amount of food ingested by mesozooplankton and the total gross primary productivity (GPP) was used as a measure of trophic transfer efficiency. We assumed that all organic carbon released by phytoplankton through primary production, egestion of unassimilated prey (mainly by protists), and natural mortality contributed to the pool of labile DOC. The contribution of different functional groups to each of the processes was

279 also investigated. Finally, the relative biomasses of mixotrophs and their respective autotrophic and
280 heterotrophic competitors were evaluated in the transition from light to nutrient limitation. Thus, a
281 third modelling experiment was conducted to simulate intermediate conditions of light and nutrient
282 limitation (I_{surf} = 100 W m^{-2} or 457 µmol photon m^{-2} s^{-1}, DIN = 16 µM nitrate).
283 *Sensitivity analyses for mixotrophic food web*
284 Sensitivity analyses were performed to evaluate how the ecological processes described
285 above (i.e. ammonium regeneration, trophic transfer efficiency, and total production of labile DOC)
286 are affected by the choice of parameter values and nutrient concentrations in the chemostat medium
287 for the mixotrophic food web. We evaluated the sensitivity of the mixotrophic food web for both the
288 nutrient-limited and the light-limited scenarios. The main parameters that define functional diversity
289 within our conceptual food web, such as those related to phototrophy, nutrient uptake, predation,
290 respiration, and mixotrophic potential (following previous sections) were selected for the analyses.
291 We used an approach based on the Monte-Carlo ensemble technique to rank the importance
292 of the input parameters (Saltelli *et al*., 2008; Sankar *et al*., 2018). This technique allows the
293 detection of the parameters (and thus of the respective processes and functional types) that each
294 targeted output is most sensitive to. Even if several input parameters are included in the analysis, a
295 few input parameters often account for most of the variation observed in model output (Saltelli *et*
296 *al*., 2008). The method generates a number *n* of realizations based on the probability density
297 functions of *m* input factors x_i (i.e. model parameters), assumed to be uniformly distributed and
298 independent from each other. Each realization produces a vector containing values randomly
299 sampled from the distributions of all input parameters. Each vector of parameters is then used to run
300 a model simulation and compute the output y. The output of *n* realizations and model runs is
301 subsequently represented by a multiple linear regression:

302 $$y = b_0 + \sum_{i=1}^{m} b_i x_i + \text{residuals} \quad (1)$$

303 The standardized regression coefficients (β_i computed from b_i) were used as global
304 sensitivity indices of the input factors (Saltelli *et al*., 2008):

305 $$\beta_i = \frac{b_i \sigma_{xi}}{\sigma_y} \quad (2)$$

306 where σ_{xi} and σ_y are the standard deviations of the realizations of the input factor x_i and of the
307 model output y, respectively. Thus, each parameter included in the analysis is associated to a
308 sensitivity coefficient which indicates whether an increase in the value of the parameter has a
309 positive or negative effect on the targeted output (i.e. increase or decrease the output value,
310 respectively). Since the validity of the results depends on the fraction of the model output variability
311 that is explained by the multiple linear regression (Saltelli *et al*., 2000), we estimated the overall

fraction of explained variance (R^2) and the significance of the standardized regression coefficients (β_i).

A total of $m = 116$ input parameters were included in the sensitivity analyses. We performed $n = 2320$ realizations assuming 20 realizations for each input parameter as a rule of thumb (Hair *et al*., 2006). Random values were generated assuming a range of ± 30% of the reference value of the input parameters (e.g. Sankar *et al*., 2018). The analyses were performed using a Python code developed for the purpose. In addition to these analyses, we conducted an extra sensitivity test to confirm that averaged model outputs during the last year of the simulation were independent from initial conditions; methods and results from this analysis can be found in the Supplementary Material. Model output and graphical visualization was processed/performed in R software (R Core Team, 2018) using the packages 'netcdf4', 'ggplot2', 'gridExtra', and 'plyr'.

Results

Light-limited scenario

Ecosystem properties differed between the non-mixotrophic and the mixotrophic food webs in the light-limited scenario (Fig. 2). Ammonium regeneration was higher in the non-mixotrophic food web, mainly due to the activity of heterotrophic protists (Fig. 2a). Once mixotrophs were included, they competed with their heterotrophic counterparts and down-regulated the biomass of heterotrophic nanoflagellates (Fig. 3). Mixotrophs did not contribute as much to the regeneration of ammonium but supported a higher trophic transfer efficiency of carbon biomass to higher trophic levels (Fig. 2b). This is explained by changes in community composition, from smaller (in the non-mixotrophic food web) to larger (in the mixotrophic food web) phototrophs, since mesozooplankton exhibit a preference for larger prey items. In the absence of mixotrophs, autotrophic nanoflagellates and microflagellates were outcompeted by picophytoplankton and diatoms (Fig. 3), with only the latter having a cell size large enough to serve as food for mesozooplankton (Fig. 2b). In the mixotrophic food web, CMs thrived, with mixotrophs contributing significantly to the diet of mesozooplankton (Fig. 2b). In turn, the production of DOC was higher in the non-mixotrophic food web (Fig. 2c). This was mainly due to the higher total GPP (Fig. S7), reflecting the high biomass levels attained by picophytoplankton and diatoms (Fig. 3), and due to higher mortality following the overall increase in carbon biomass (Fig. S8). Relative to that of phototrophs, the production of DOC by phagotrophic protists was minor in the non-mixotrophic framework while being more significant in the presence of mixotrophs (Fig. 2c).

Nutrient-limited scenario

Mixotrophy was more successful under the high-light and low-nutrient condition, with mixotrophs outcompeting their strict autotrophic and strict heterotrophic counterparts, respectively (Fig. 3). As a result, ecosystem properties differed substantially between the non-mixotrophic and the mixotrophic food webs in this scenario (Figs. 3 and 4). Similar to the light limited-scenario, ammonium regeneration was lower in the mixotrophic food web (Fig. 4a) and NCMs could outcompete their heterotrophic counterparts due to limited prey availability (Fig. 3). As mixotrophs did not contribute to the regeneration of ammonium (Fig. 4a), this in turn decreased the availability of inorganic nutrients, which favoured CMs (mainly CM-nano) over strict autotrophs (Fig. 3).

The role of mixotrophy in the trophic transfer efficiency was even more pronounced in the nutrient-limited scenario (Fig. 4b). Indeed, while in the non-mixotrophic food web mesozooplankton was limited by the paucity of suitable prey, in the mixotrophic food web, mesozooplankton could rely on NCMs which in turn were supported by the CM-nano biomass feeding on picophytoplankton (Figs. 3 and 4b). Contrary to the light-limited scenario, mixotrophy also boosted the production of labile DOC under nutrient limitation. This was mainly related to a greater fraction of ingested prey remaining unassimilated (i.e. more inefficient predators due to lower prey quality). The main contributors to the production of labile DOC on this scenario were CM-nano and GNCMs (Fig. 4c). The direct effect of increased availability of labile DOC is the stimulation of bacterial metabolism, which in turn leads to enhanced production of recalcitrant DOC (Fig. 4c). Accordingly, production of recalcitrant DOC was considerably lower in the non-mixotrophic food web (Fig. 4c).

The individual and additional effects of mixotrophic diversity were also investigated by including one or more mixotrophic types at a time (Fig. S9). The additional simulations were performed under nutrient limitation due to the higher importance of mixotrophy on this scenario. We evaluated the changes on community structure (in terms of carbon biomass considering mixotrophs and their strict auto- and hetero- trophic competitors), ammonium regeneration, and trophic transfer efficiency relative to the non-mixotrophic food web. When only one mixotrophic type was considered, changes on community structure were more significant for CM-nano which, outcompeting picophytoplankton, were the only mixotrophic type to enable the growth of mesozooplankton alone (Fig. S9). On the other hand, CM-micro down-regulated the biomass of strict heterotrophs, allowing higher picophytoplankton biomass and decreasing the overall regeneration of ammonium by ~ 70% (Fig. S9). The individual impact of GNCMs or SNCMs was small; in fact, SNCMs did not survive because they depend on nanophytoplankton to obtain their phototrophic capacity and this group was outcompeted by picophytoplankton (Fig. S9). Differences were more pronounced once CM-nano and GNCMs or SNCMs were included in the model because

CM-nano supports the biomass of NCMs which, in turn, is transferred to mesozooplankton (Fig. S9). Finally, including all mixotrophic types increased the extent of the overall niche for mixotrophy, enhancing its overall impact (Fig. S9).

Sensitivity analyses for mixotrophic food web

The overall fraction of variance explained by the multiple linear regression on the 116 selected parameters was high for all three targeted outputs in both limitation scenarios ($R^2 > 0.9$). Here we present the first 8 parameters ranked by highest sensitivity (Tables II and III); the full ranking can be found in the supplementary material (Table S6). The sensitivity coefficients of all the parameters reported here were statistically significant. A positive coefficient (in Tables II and III) indicates that an increase in the parameter value led to an increase in the output value and vice-versa.

In the light-limited scenario, all targeted outputs were most sensitive to photosynthetic parameters (Table II). Ammonium regeneration was promoted by increasing the efficiency of diatoms and picophytoplankton in harvesting light (α_{Chl} and $ChlC_{abs}$, positive coefficients in Table II) and decreased if higher maximum nitrogen to carbon quotas were considered (NC_{max}, negative coefficients in Table II). In turn, the trophic transfer efficiency was most sensitive to the optimal prey size (S_{opt}) of CM-nano (Table II). Increasing their optimal prey size increased the intraguild predation within this group, resulting in higher growth rates but lower population biomass. A cascade effect is then observed, because less prey would be available for CM-micro, which are an important prey item for mesozooplankton in this scenario ($Cr_{CM\text{-}micro}$). On the other hand, increasing α_{Chl} and $ChlC_{abs}$ among CMs and diatoms supported higher trophic transfer efficiency, since these were the main prey supporting mesozooplankton biomass (positive coefficients in Table II). Mesozooplankton intraguild predation ($Cr_{mesozoo}$) was also important and negatively impacted (i.e. decreased) the trophic transfer efficiency (ranked 5th). Regarding the production of labile DOC, the contribution of the major phototrophs (diatoms, picophytoplankton, and CM-nano) was the main source of DOC in the light-limited scenario, mainly driven by parameters controlling their phototrophic potential (α_{Chl} and $ChlC_{abs}$; positive coefficients in Table II). The optimal prey size of CM-nano was also important, although to a lesser extent (S_{opt}).

In the nutrient-limited scenario, the parameterisation of bacteria and mixotrophs was more important (Table III). Ammonium regeneration was negatively impacted by increasing the maximum prey size accessible by CM-nano (S_{max}), as well as its preferred prey size (S_{opt}) (negative coefficients in Table III), because it favours the success of CM-nano relative to their strict heterotrophic competitors. However, increases in the maximum phototrophic growth rate (μ_{phot}) of

CM-nano counterbalanced the negative effect of S_{opt}. Maximum internal N or P to carbon quotas were also important (ranked 2nd, 3rd, and 8th). Similar to the light-limited scenario, the trophic transfer efficiency was inversely related to the optimal prey size (S_{opt}) of CM-nano, resulting in less prey for GNCMs, which were an important prey for mesozooplankton under nutrient limitation (ranked 1st and 3rd, respectively). A similar negative effect was observed when increasing S_{max} among mixotrophs (negative coefficients in Table II). Parameters associated with picophytoplankton and bacteria were also important (μ_{phot} and NC_{max}, respectively), but to a lesser extent than the previous ones (Table III). The production of labile DOC was positively related (i.e. increased) with the maximum phototrophic growth rate of CM-nano (μ_{phot}) and with parameters controlling the predation by NCMs (S_{max}; positive coefficients in Table II). The internal stoichiometry regulation of mixotrophs and bacteria was also important, with a negative effect associated with N to C ratios (ranked 3rd, 4th, and 6th) and a positive effect associated with P to C ratios (ranked 7th and 8th).

Discussion

Our study suggests that the interpretations and predictions of the functioning of the marine planktonic ecosystem could radically change if we consider mixotrophic functional diversity in ocean models, with mixotrophy impacting nutrient availability, mass and energy transfer to higher trophic levels, and the microbial loop (Figs. 2–4). Our simulations show that the relative dominance of different mixotrophic functional groups can shape the planktonic ecosystem in different ways depending on light and nutrient regimes. Size was shown to be important to determine the success of mixotrophs with an innate capacity for photosynthesis; while small cells dominated under nutrient limitation, larger cells were more important under light limitation (Fig. 5a). Among acquired phototrophs, the specificity of the prey from which kleptochloroplasts are obtained affected their success, with generalist forms dominating under nutrient limitation and specialist forms showing maximal contribution in intermediate conditions of light and nutrients and under nutrient limitation (Fig. 5b).

The results from our simulations appear consistent with empirical observations. The nano-CMs and GNCMs (e.g. oligotrich ciliates) have been reported to be important members within oligotrophic gyres and during summer within temperate seas (Stoecker *et al*., 1987; Zubkov and Tarran, 2008; Hartmann *et al*., 2012; Unrein *et al*., 2014; Haraguchi *et al*., 2018). In contrast, micro-CMs and SNCMs (e.g. *Mesodinium rubrum*) can be major components of plankton assemblages in eutrophic coastal environments and during winter within temperate seas (Burkholder *et al*., 2008; Jeong *et al*., 2010, Hansen, 2011; Johnson *et al*., 2013). Our simulations also produced realistic estimates of the biomass ratios between NCMs and their heterotrophic competitors. In the light-

447 limited scenario, our model predicted coexistence of NCMs and their heterotrophic counterparts,
448 with the latter comprising half of the total assemblage (Fig. 5b). These results were consistent with
449 previous observations showing that strict heterotrophs comprise on average 60% of total ciliate
450 biomass during winter within coastal temperate seas (Nielsen and Kiørboe, 1994; Leles *et al*.,
451 2017). Once limited by prey availability, strict heterotrophs survived at a very low biomass only
452 accounting for 5% of the total assemblage (Fig. 5b). Overall, this value is lower than expected
453 during summer (Leles *et al*., 2017); minimum values were reported in the Mediterranean Sea and in
454 the Northwest Atlantic Shelves, in which heterotrophic microzooplankton accounted for less than
455 15% of total ciliate biomass (Stoecker *et al*. 1987; Modigh, 2001; Bernard and Rassoulzadegan,
456 1994).

457 Acquired phototrophy has been suggested to stabilise coexistence between NCMs and the
458 prey that provides their phototrophic potential (Moeller *et al*., 2016). However, the nature of this
459 coexistence would depend on light availability, with the amplitude of repeating biomass cycles
460 increasing with irradiance (Moeller *et al*., 2016). In a food web considering bottom-up (nutrients)
461 and top-down (higher predators) controls, we found that the amplitude of repeating cycles was
462 considerably lower under high-light and low-nutrient conditions, approaching a constant steady-
463 state (Fig. S3). In addition, when we assumed trophic interactions between SNCMs, GNCMs, and
464 strict heterotrophs; the model became more unstable with one group slowly outcompeting the
465 others. Defining the differences between these groups is challenging. For instance, experimental
466 evidence found similar maximum growth rates and inorganic N uptake between strict heterotrophs
467 and GNCMs (Schoener and McManus, 2017). Although our assumptions were based on the current
468 literature, there is little quantitative information on the costs and benefits associated to acquired
469 phototrophy (Dolan and Pérez, 2000; Stoecker *et al*., 2009; McManus *et al*., 2012). Our sensitivity
470 experiments suggest that defining the prey size spectrum accessible and selected by each of these
471 groups significantly impact the targeted outputs (Tables II and III).

472 Our model predicted that the dominance of mixotrophs over their strict autotrophic and
473 heterotrophic counterparts increases in the transition from light to nutrient limitation (Fig. 5).
474 Mixotrophs can outcompete strict autotrophs and strict heterotrophs by using nutrients more
475 efficiently. Indeed, when nutrient-rich prey are ingested any surplus of N and P may be combined
476 with newly fixed carbon instead of being excreted outside the cell (Rothhaupt, 1997; Flynn and
477 Mitra, 2009; Fischer *et al*., 2016). In addition, certain species of acquired phototrophs can take up
478 inorganic nutrients (Hattenrath-Lehmann and Gobler, 2015; Qiu *et al*., 2016). These features
479 minimise the remineralization of nutrients to the environment enhancing the bottom-up control of
480 strict autotrophs under nutrient limitation and favouring mixotrophs over strict heterotrophs under
481 low prey availability (Fig. 5). Thus, the simulations indicate that the presence of not only CMs but

also NCMs can decrease nutrient regeneration. This is consistent with previous findings showing that the dinoflagellate *Dinophysis acuminata* and the ciliate *M. rubrum* take up inorganic nutrients; these two species are classifiable as SNCMs as they must acquire kleptochloroplasts from *M. rubrum* and red cryptophyte algal prey, respectively (Hattenrath-Lehmann and Gobler, 2015; Qiu *et al*., 2016). Recent evidence also shows that oligotrich ciliates (i.e. GNCMs) can take up inorganic nutrients, although it might not contribute significantly to their growth (Schoener and McManus, 2017).

Mixotrophs have been previously suggested to increase the trophic transfer efficiency to higher trophic levels (Stoecker *et al*., 2009; Stoecker *et al*., 2017). Our simulations support and expand this ecological concept by considering the functional diversity among mixotrophs and their strict autotrophic and heterotrophic competitors. Our results suggest that CMs have a competitive advantage over strict autotrophic competitors, particularly under nutrient limitation, allowing the accumulation of biomass in larger prey instead of in pico-sized prey, which are too small to be consumed by higher consumers. In turn, CMs provide photosynthetic potential to NCMs, which composed the bulk of biomass that sustained higher trophic levels (Fig. 4b). In fact, crustacean zooplankton and fish larvae preferentially prey on NCMs, such as oligotrich ciliates and *M. rubrum,* rather than on their strict auto- and hetero- trophic competitors (Broglio *et al*., 2004; Figueiredo *et al*., 2007). Our simulations suggest that ~ 50% of mesozooplankton diet was composed by NCMs in the nutrient-limited scenario versus 20% under light limitation. These values are consistent with observations showing that the relative importance of the consumption of NCMs by copepods varies across environmental gradients, increasing towards less productive systems (Calbet and Saiz, 2005).

Mixed nutrition may also increase the release of labile DOC among protists (Flynn *et al*., 2008; Mitra *et al*., 2014). The theoretical framework presented here provides a platform to explore how this might affect the production of recalcitrant DOC by bacteria. Our results showed higher production of labile DOC in the mixotrophic food web only when nutrients were limiting, stimulating bacterial production (Mitra *et al*., 2014) and, consequently, boosting the production of recalcitrant DOC (Fig. 2c vs Fig. 4c). The main source responsible for the higher production of labile DOC on this scenario was the increased release of labile DOC by protists (Fig. S8). This release, in turn, was induced by higher prey consumption combined with an overall poor prey quality, described here by internal N:C and P:C quotas (Mitra, 2006; Polimene *et al*., 2015). Overall, the stronger nutrient limitation in the presence of mixotrophs resulted in lower prey quality and hence less efficient microzooplankton. However, it is noteworthy that the production of labile DOC and hence of recalcitrant DOC is strongly dependent on model assumptions, particularly in the partitioning of voided material between particulate and dissolved pools. It is also important to note that our model lacked the description of osmotrophy among CMs (Ghyoot *et al*., 2017), which

517 can decrease the net production of DOC, or even change the mixotroph from a source of DOC into
518 a sink.
519 Our results are dependent on several assumptions and uncertain parameters, but we aimed to
520 explore the emerging paradigm in marine ecology, in which the phytoplankton-zooplankton
521 dichotomy no longer holds. Constitutive mixotrophy was particularly important to maintain
522 phototrophy within nano- and micro- plankton size classes, which would be outcompeted by
523 picophytoplankton otherwise. This result appears robust because it is mainly related to the overall
524 predation impact, which is lower among picophytoplankton as predicted by allometric constraints.
525 The success of different phototrophs is also dependent on their phototrophic capacities and internal
526 stoichiometric quotas, as showed by our sensitivity tests, and these parameters are well
527 characterised in the literature (Table S3). On the other hand, acquired phototrophs were too
528 dominant relative to their heterotrophic competitors in our simulations. While we could compile
529 information on their total prey size spectrum (Table S1), it seems that we still lack information on
530 the costs associated to acquired phototrophy. Our results also suggest that NCMs may act as a sink
531 or source of inorganic nutrients, depending on environmental conditions. Similarly, quantitative
532 studies on the cycling of DOM by mixotrophs and consequently in the production of recalcitrant
533 DOC by bacteria, can help to elucidate the significance of mixotrophy to the microbial carbon
534 pump.
535 The importance of mixotrophy in the environmental setups used in our simulation
536 experiments can have profound consequences in view of climatic and anthropogenic changes on the
537 oceans, particularly in oligotrophic seas and eutrophic coastal systems. Warmer waters and stronger
538 stratification have been previously hypothesised to favour mixotrophic plankton in oligotrophic seas
539 (Polovina *et al*., 2008; Wilken *et al*., 2013; Behrenfeld *et al*., 2016). In turn, increased
540 eutrophication in coastal waters can induce light-limitation and promote the formation of harmful
541 algal blooms, many of which are mixotrophic species (Burkholder *et al*., 2008; Gomes *et al*., 2014).
542 Our findings provide the basis for the mechanisms giving competitive advantages to different
543 mixotrophs relative to their strict auto- and hetero- trophic competitors under such environmental
544 conditions (i.e. nutrient or light limitation). In view of our results, we believe that future studies
545 aiming to predict the impact of environmental changes on the oceanic food webs should consider
546 the mixotrophic potential of plankton communities.
547
548 **Conclusions**
549 Our investigation suggests that mixotrophic functional diversity can significantly alter our
550 understanding of ecosystem dynamics within the lower trophic levels of marine food webs, with
551 key groups of mixotrophs controlling nutrient regulation, trophic transfer, and the microbial loop.

552 Our model predicted predominance of nano-CMs and GNCMs in nutrient depleted conditions (akin
553 to oligotrophic oceans), and a higher importance of micro-CMs and SNCMs under light limited
554 conditions (e.g. eutrophic coastal systems). This is the first time that the roles of different mixotroph
555 types have been explored simultaneously within plankton food webs. This work demonstrates the
556 importance of deploying detailed descriptions of mixotroph physiology. Our results also show how
557 mixotrophy interacts in the direct and indirect control of the growth of strict autotrophic and
558 heterotrophic populations, particularly under nutrient limitation. Moreover, we demonstrated how
559 mixotrophy can promote the transfer of carbon biomass to higher planktonic predators through the
560 interplay between CMs and NCMs. Critically, we have constructed a food web framework for
561 comprehensive quantitative exploration of the role of mixotrophic functional diversity in marine
562 ecosystems, which can be readily implemented in a variety of settings: from chemostats to spatially
563 structured models of the water column (1D) and the global ocean (3D). It thus provides a powerful
564 tool to investigate the role of mixotrophy in a changing ocean.
565
566 **Acknowledgements**
567 The authors thank three anonymous reviewers and the marine ecosystem modelling group at PML
568 which provided valuable feedback and discussion, particularly Sévrine Sailley, which provided
569 valuable comments on data visualization.
570
571 **Funding**
572 S.G.L was supported by the Brazilian government programme *Science Without Borders* through
573 CNPq (Conselho Nacional de Desenvolvimento Científico e Tecnológico - Brasil). The work of
574 J.Br. was supported by the Natural Environment Research Council (NERC) and Department for
575 Environment, Food and Rural Affairs [grant number NE/L003066/1, Marine Ecosystems Research
576 Programme] and NERC National Capability in Marine Modelling. J. Bl. and L.P. were supported by
577 the NERC National Capability in Marine Modelling and by the NERC grant NE/R011087/1 (L.P.).
578 S.C. was supported by the NERC National Centre for Earth Observation (NCEO). The origins of
579 this work were funded by grants to K.J.F and A.M. from the Leverhulme Trust (International
580 Network Grant F00391 V) and NERC (UK) through its iMAR-NET programme.
581
582 **References**
583 Anderson, R., Jürgens, K. and Hansen, P.J. (2017) Mixotrophic phytoflagellate bacterivory field
584 measurements strongly biased by standard approaches: a case study. *Front. Microbiol.*, **8**, 1–
585 12.

586 Araújo, M.S., Bolnick, D.I. and Layman, C.A. (2011) The ecological causes of individual
587 specialisation. *Ecol. Lett.*, **14**, 948–958.

Baretta-Bekker, J.G., Baretta, J.W. & Koch Rasmussen, E. (1995) The microbial food web in the European Regional Seas Ecosystem Model. *Netherlands J. Sea Res.*, **33**, 363–379.

Behrenfeld, M.J., O'Malley, R.T., Boss, E.S., Westberry, T.K., Graff, J.R., Halsey, K.H., *et al.* (2016) Revaluating ocean warming impacts on global phytoplankton. *Nat. Clim. Chang.*, **6**, 323–330.

Bernard, C. and Rassouladegan, F. (1994) Seasonal variations of mixotrophic ciliates in the northwest Mediterranean Sea. *Mar. Ecol. Prog. Ser.*, **108**, 295–302.

Biard, T., Stemmann, L., Picheral, M., Mayot, N., Vandromme, P., Hauss, H., Gorsky, G., Guidi, L., Kiko, R. and Not, F. (2016) *In situ* imaging reveals the biomass of giant protists in the global ocean. *Nature*, **532**, 504–507.

Broglio, E., Saiz, E., Calbet, A., Trepat, I. and Alcaraz, M. (2004) Trophic impact and prey selection by crustacean zooplankton on the microbial communities of an oligotrophic coastal area (NW Mediterranean Sea). *Aquat. Microb. Ecol.*, **35**, 65–78.

Bruggeman, J. and Bolding, K. (2014) A general framework for aquatic biogeochemical models. *Environ. Model. Softw.*, **61**, 249–265.

Burkholder, J.M., Glibert, P.M. and Skelton, H.M. (2008) Mixotrophy, a major mode of nutrition for harmful algal species in eutrophic waters. *Harmful Algae*, **8**, 77–93.

Butenschön, M., Clark, J., Aldridge, J.N., Icarus Allen, J., Artioli, Y., Blackford, J., *et al.* (2016) ERSEM 15.06: A generic model for marine biogeochemistry and the ecosystem dynamics of the lower trophic levels. *Geosci. Model Dev.*, **9**, 1293–1339.

Calbet, A. and Saiz, E. (2005) The ciliate-copepod link in marine ecosystems. *Aquat. Microb. Ecol.*, **38**, 157–167.

Cloern, J. and Dufford, R. (2005) Phytoplankton community ecology: Principles applied in San Francisco Bay. *Mar. Ecol. Prog. Ser.*, **285**, 11–28.

Dolan, J.R. and Pérez, M.T. (2000) Costs, benefits and characteristics of mixotrophy in marine oligotrichs. *Freshw. Biol.*, **45**, 227–238.

Figueiredo, G.M., Nash, R.D.M. and Montagnes, D.J.S. (2007) Do protozoa contribute significantly to the diet of larval fish in the Irish Sea? *J. Mar. Biol. Assoc. United Kingdom*, **87**, 843–850.

Fischer, R., Giebel, H.A., Hillebrand, H. and Ptacnik, R. (2016) Importance of mixotrophic bacterivory can be predicted by light and loss rates. *Oikos*, **126**, 713–722.

Flynn, K.J. (2005) Incorporating plankton respiration in models of aquatic ecosystem function. In: *Respiration in Aquatic Ecosystems* (eds. del Giorgio, P. and Williams, P.J. le B.). Oxford University Press, New York, pp. 248–266.

Flynn, K.J. (2018) *Dynamic Ecology – an introduction to the art of simulating trophic dynamics*. Swansea University, UK.

Flynn, K.J., Clark, D.R. and Xue, Y. (2008) Modeling the release of dissolved organic matter by phytoplankton. *J. Phycol.*, **44**, 1171–1187.

Flynn, K.J. and Hansen, P.J. (2013) Cutting the canopy to defeat the "selfish gene"; conflicting selection pressures for the integration of phototrophy in mixotrophic protists. *Protist*, **164**, 811–23.

Flynn, K.J. and Martin-Jézéquel, V. (2000) Modelling Si-N limited growth of diatoms. *J. Plankton Res.*, **22**, 447–472.

630 Flynn, K.J. and Mitra, A. (2009) Building the "perfect beast": Modelling mixotrophic plankton. *J.*
631 *Plankton Res.*, **31**, 965–992.

632 Flynn, K.J. and Mitra, A. (2016) Why plankton modelers should reconsider using rectangular
633 hyperbolic (Michaelis-Menten, Monod) descriptions of predator-prey interactions. *Front. Mar.*
634 *Sci.*, **3**, 165.

635 Flynn, K.J., Stoecker, D.K., Mitra, A., Raven, J. a., Glibert, P.M., Hansen, P.J., *et al.* (2013) Misuse
636 of the phytoplankton – zooplankton dichotomy : the need to assign organisms as mixotrophs
637 within plankton functional types. *J. Plankton Res.*, **35**, 3–11.

638 Ghyoot, C., Lancelot, C., Flynn, K.J., Mitra, A. and Gypens, N. (2017) Introducing mixotrophy into
639 a biogeochemical model describing an eutrophied coastal ecosystem: The Southern North Sea.
640 *Prog. Oceanogr.*, **157**, 1–11.

641 Gomes, H. do R., Goes, J.I., Matondkar, S.G.P., Buskey, E.J., Basu, S., Parab, S., *et al.* (2014)
642 Massive outbreaks of *Noctiluca scintillans* blooms in the Arabian Sea due to spread of
643 hypoxia. *Nat. Commun.*, **5**, 4862.

644 Granados, M., Duffy, S., McKindsey, C.W. and Fussmann, G.F. (2017) Stabilizing mechanisms in a
645 food web with an introduced omnivore. *Ecol. Evol.*, **7**, 5016–5025.

646 Gustafson, D.E., Stoecker, D.K., Johnson, M.D., Van Heukelem, W.F. and Sneider, K. (2000)
647 Cryptophyte algae are robbed of their organelles by the marine ciliate *Mesodinium rubrum*.
648 *Nature*, **405**, 1049–1052.

649 Hansell, D.A. (2013) Recalcitrant Dissolved Organic Carbon Fractions. *Ann. Rev. Mar. Sci.*, **5**,
650 421–445.

651 Hansen, P.J. (2011) The Role of Photosynthesis and Food Uptake for the Growth of Marine
652 Mixotrophic Dinoflagellates1. *J. Eukaryot. Microbiol.*, **58**, 203–214.

653 Haraguchi, L., Jakobsen, H.H., Lundholm, N. and Carstensen, J. (2018) Phytoplankton Community
654 Dynamics: A Driver for Ciliate Trophic Strategies. *Front. Mar. Sci.*, **5**, 272.

655 Hartmann, M., Grob, C., Tarran, G.A., Martin, A.P., Burkill, P.H. and Scanlan, D.J. (2012)
656 Mixotrophic basis of Atlantic oligotrophic ecosystems. *Proc. Natl. Acad. Sci.*, **109**, 5756–
657 5760.

658 Hattenrath-Lehmann, T. and Gobler, C.J. (2015) The contribution of inorganic and organic nutrients
659 to the growth of a North American isolate of the mixotrophic dinoflagellate, *Dinophysis*
660 *acuminata*. *Limnol. Oceanogr.*, **60**, 1588–1603.

661 Hunter, M.D. and Price, P.W. (1992) Playing chutes and ladders : heterogeneity and the relative
662 roles of bottom-up and top- down forces in natural communities. *Ecology*, **73**, 724–732.

663 Jeong, H.J., Yoo, Y. Du, Kim, J.S., Seong, K.A., Kang, N.S. and Kim, T.H. (2010) Growth, feeding
664 and ecological roles of the mixotrophic and heterotrophic dinoflagellates in marine planktonic
665 food webs. *Ocean Sci. J.*, **45**, 65–91.

666 Jiao, N., Herndl, G.J., Hansell, D.A., Benner, R., Kattner, G., Wilhelm, S.W., *et al.* (2010)
667 Microbial production of recalcitrant dissolved organic matter: Long-term carbon storage in the
668 global ocean. *Nat. Rev. Microbiol.*, **8**, 593–599.

669 Johnson, M.D. (2011) Acquired phototrophy in ciliates: A review of cellular interactions and
670 structural adaptations. *J. Eukaryot. Microbiol.*, **58**, 185–195.

671 Johnson, M.D., Oldach, D., Delwiche, C.F. and Stoecker, D.K. (2007) Retention of transcriptionally
672 active cryptophyte nuclei by the ciliate *Myrionecta rubra*. *Nature*, **445**, 426–428.

673 Johnson, M.D., Stoecker, D.K. and Marshall, H.G. (2013) Seasonal dynamics of *Mesodinium*
674 *rubrum* in Chesapeake Bay. *J. Plankton Res.*, **35**, 877–893.

675 Johnson, P.T.J., Dobson, A., Lafferty, K.D., Marcogliese, D.J., Memmott, J., Orlofske, S.A., *et al.*
676 (2010) When parasites become prey: Ecological and epidemiological significance of eating
677 parasites. *Trends Ecol. Evol.*, **25**, 362–371.

678 Legendre, L., Rivkin, R.B., Weinbauer, M.G., Guidi, L. and Uitz, J. (2015) The microbial carbon
679 pump concept: Potential biogeochemical significance in the globally changing ocean. *Prog.*
680 *Oceanogr.*, **134**, 432–450.

681 Leles, S.G., Mitra, A., Flynn, K.J., Stoecker, D.K., Hansen, P.J., Calbet, A., *et al.* (2017) Oceanic
682 protists with different forms of acquired phototrophy display contrasting biogeographies and
683 abundance. *Proc. R. Soc. B*, **284**, 20170664.

684 McManus, G.B., Schoener, D.M. and Haberlandt, K. (2012) Chloroplast symbiosis in a marine
685 ciliate: ecophysiology and the risks and rewards of hosting foreign organelles. *Front.*
686 *Microbiol.*, **3**, 321.

687 Mitra, A. (2006) A multi-nutrient model for the description of stoichiometric modulation of
688 predation in micro- and mesozooplankton. *J. Plankton Res.*, **28**, 597–611.

689 Mitra, A. & Flynn, K.J. (2010) Modelling mixotrophy in harmful algal blooms: More or less the
690 sum of the parts? *J. Mar. Syst.*, **83**, 158–169.

691 Mitra, A., Flynn, K.J., Burkholder, J.M., Berge, T., Calbet, A., Raven, J.A., *et al.* (2014) The role of
692 mixotrophic protists in the biological carbon pump. *Biogeosciences*, **11**, 995–1005.

693 Mitra, A., Flynn, K.J., Tillmann, U., Raven, J.A., Caron, D., Stoecker, D.K., *et al.* (2016) Defining
694 Planktonic Protist Functional Groups on Mechanisms for Energy and Nutrient Acquisition:
695 Incorporation of Diverse Mixotrophic Strategies. *Protist*, **167**, 106–120.

696 Modigh, M. (2001) Seasonal variations of photosynthetic ciliates at a Mediterranean coastal site.
697 *Aquat. Microb. Ecol.*, **23**, 163–175.

698 Moeller, H. V., Peltomaa, E., Johnson, M.D. and Neubert, M.G. (2016) Acquired phototrophy
699 stabilises coexistence and shapes intrinsic dynamics of an intraguild predator and its prey.
700 *Ecol. Lett.*, **19**, 393–402.

701 Nielsen, T.G. and Kiørboe, T. (1994) Regulation of zooplankton biomass and production in a
702 temperate, coastal ecosystem. 2. Ciliates. *Limnol. Oceanogr.*, **39**, 508–519.

703 Polimene, L., Sailley, S., Clark, D., Mitra, A. and Allen, J.I. (2017) Biological or microbial carbon
704 pump? The role of phytoplankton stoichiometry in ocean carbon sequestration. *J. Plankton*
705 *Res.*, **39**, 180–186.

706 Polimene, L., Mitra, A., Sailley, S.F., Ciavatta, S., Widdicombe, C.E., Atkinson, A. and Allen, J.I.
707 (2015) Decrease in diatom palatability contributes to bloom formation in the Western English
708 Channel. *Prog. Oceanogr.*, **137**, 484–497.

709 Polis, G.A., Myers, C.A. and Holt, R.D. (1989) The Ecology and Evolution of Intraguild Predation :
710 Potential Competitors That Eat Each Other Author (s): Gary A . Polis , Christopher A . Myers
711 and Robert D . Holt Source : Annual Review of Ecology and Systematics , Vol . 20 (1989),
712 pp . 297-330 Publ. *Annu. Rev. Ecol. Syst.*, **20**, 297–330.

713 Polovina, J.J., Howell, E.A. and Abecassis, M. (2008) Ocean's least productive waters are
714 expanding. *Geophys. Res. Lett.*, **35**, 2–6.

715 Qiu, D., Huang, L. and Lin, S. (2016) Cryptophyte farming by symbiotic ciliate host detected in

situ. *Proc. Natl. Acad. Sci.*, **113**, 12208–12213.

R Core Team (2018) R: a language and environment for statistical computing. Vienna, Austria: R Foundation for Statistical Computing.

Rothhaupt, K.O. (1997) Nutrient turnover by freshwater bacterivorous flagellates: Differences between a heterotrophic and a mixotrophic chrysophyte. *Aquat. Microb. Ecol.*, **12**, 65–70.

Saltelli, A., Chan, K. and Scott, M. (2000) *Sensitivity Analysis. Wiley Series in Probability and Statistics*. John Wiley and Sons, Ltd., New York.

Saltelli, A., Ratto, M., Andres, T., Campolongo, F., Cariboni, J., Gatelli, D., *et al.* (2008) *Global Sensitivity Analysis. The Primer*. *Glob. Sensit. Anal. Prim.* John Wiley and Sons Ltd, Chichester, UK.

Sankar, S., Polimene, L., Marin, L., Menon, N.N., Samuelsen, A., Pastres, R., *et al.* (2018). Sensitivity of the simulated Oxygen Minimum Zone to biogeochemical processes at an oligotrophic site in the Arabian Sea. *Ecol. Modell.*, **372**, 12–23.

Schoener, D.M. and McManus, G.B. (2017) Growth, grazing, and inorganic C and N uptake in a mixotrophic and a heterotrophic ciliate. *J. Plankton Res.*, **39**, 379–391.

Selosse, M.-A., Charpin, M. and Not, F. (2017) Mixotrophy everywhere on land and in water: the grand écart hypothesis. *Ecol. Lett.*, **20**, 246–263.

Stickney, H.L., Hood, R.R. and Stoecker, D.K. (2000) The impact of mixotrophy on planktonic marine ecosystems. *Ecol. Modell.*, **125**, 203–230.

Stoderegger, K. and Herndl, G.J. (1998) Production and release of bacterial capsular material and its subsequent utilization by marine bacterioplankton. *Limnol. Oceanogr.*, **43**, 877–884.

Stoecker, D., Hansen, P., Caron, D. and Mitra, A. (2017) Mixotrophy in the marine plankton. *Ann. Rev. Mar. Sci.*, **9**, 311–335.

Stoecker, D.K., Johnson, M.D., De Vargas, C. and Not, F. (2009) Acquired phototrophy in aquatic protists. *Aquat. Microb. Ecol.*, **57**, 279–310.

Stoecker, D.K., Michaels, A.E. and Davis, L.H. (1987) Large proportion of marine planktonic ciliates found to contain functional chloroplasts. *Nature*, **326**, 790–792.

Stoecker, D.K., Silver, M.W., Michaels, A.E. and Davis, L.H. (1988-1989) Enslavement of algal chloroplasts by four Strombidium spp. (Ciliophora, Oligotrichida). *Mar. Microb. Food Webs*, **3**, 79–100.

Thingstad, T.F., Havskum, H., Garde, K. and Riemann, B. (1996) On the strategy of "eating your competitor": a mathematical analysis of algal mixotrophy. *Ecology*, **77**, 2108–2118.

Tittel, J., Bissinger, V., Zippel, B., Gaedke, U., Bell, E., Lorke, A., *et al.* (2003) Mixotrophs combine resource use to outcompete specialists: implications for aquatic food webs. *Proc. Natl. Acad. Sci. U. S. A.*, **100**, 12776–12781.

Unrein, F., Gasol, J.M., Not, F., Forn, I. and Massana, R. (2014) Mixotrophic haptophytes are key bacterial grazers in oligotrophic coastal waters. *ISME J.*, **8**, 164–176.

Våge, S., Castellani, M., Giske, J. and Thingstad, T.F. (2013) Successful strategies in size structured mixotrophic food webs. *Aquat. Ecol.*, **47**, 329–347.

Williams, R.J. and Martinez, N.D. (2000) Simple rules yield complex foodwebs. *Nature*, **404**, 180–183.

757 Wilken, S., Huisman, J., Naus-Wiezer, S. and Van Donk, E. (2013) Mixotrophic organisms become
758 more heterotrophic with rising temperature. *Ecol. Lett.*, **16**, 225–233.

759 Worm, B., Lotze, H.K., Hillebrand, H. and Sommer, U. (2002) Consumer versus resource control of
760 species diversity and ecosystem functioning. *Nature*, **417**, 848–851.

761 Zubkov, M. V and Tarran, G.A. (2008) High bacterivory by the smallest phytoplankton in the North
762 Atlantic Ocean. *Nature*, **455**, 224–226.

763

Figures

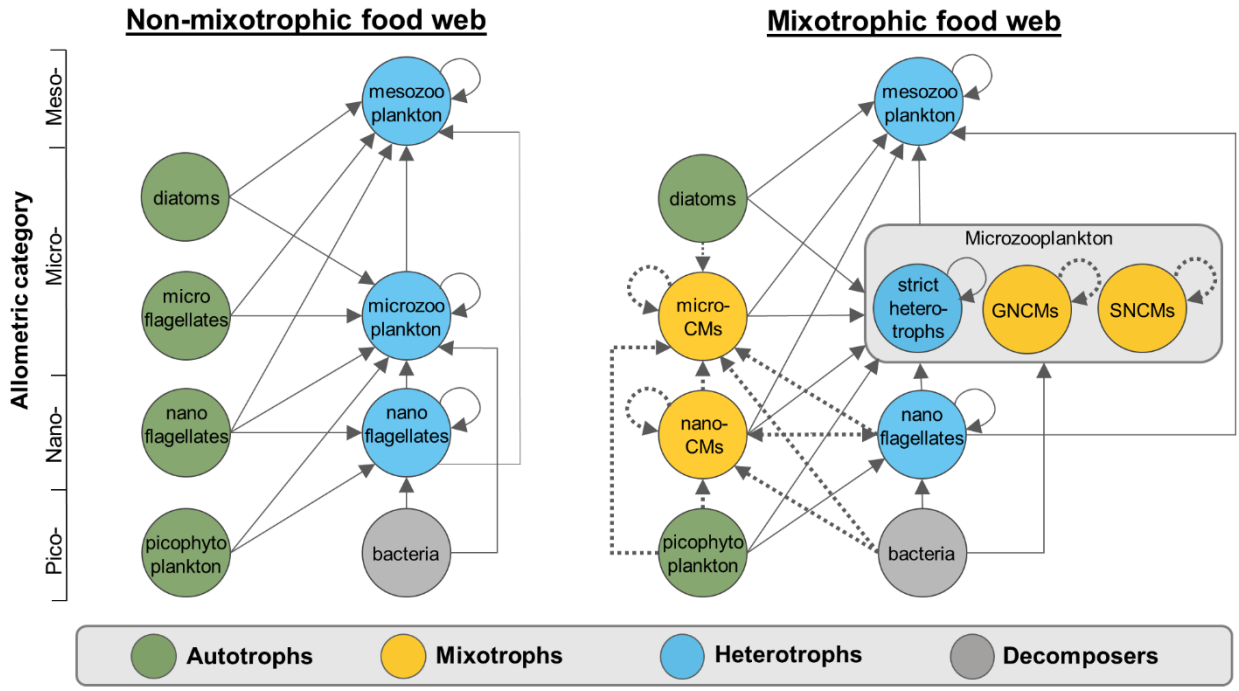

Fig. 1 Conceptual frameworks of plankton food webs used on this study to investigate the impact of mixotrophic diversity on different ecosystem properties. Food webs only differ in the presence of the mixotrophic trait. Arrows indicate trophic interactions; dotted arrows correspond to new interactions associated to mixotrophy. Abbreviations are as per Table I.

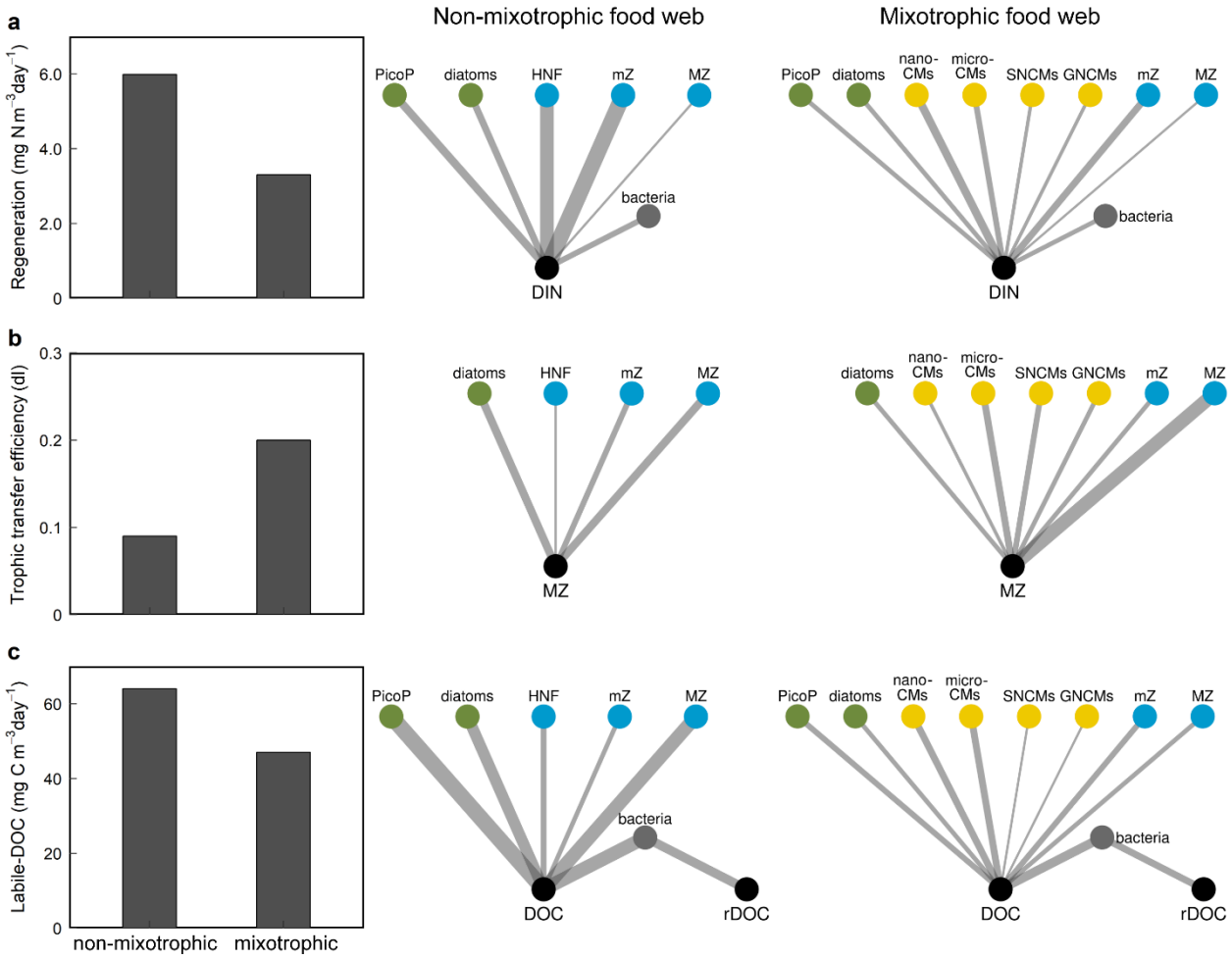

Fig. 2 Light limited-scenario for the non-mixotrophic and the mixotrophic food webs. a) ammonium (DIN) regeneration; b) trophic transfer efficiency (measured by the ratio of the total amount of food ingested by mesozooplankton (MZ) by the total gross primary productivity); and c) total production of labile dissolved organic carbon (DOC). Data were averaged for the last year of simulation. Schematics show the relative contribution of functional groups (green–autotrophs, yellow–mixotrophs, blue–heterotrophs, grey–decomposers) to each of the ecosystem properties (black nodes). In panel b, fluxes represent the amount of food ingested by mesozooplankton. rDOC–recalcitrant DOC, dl-dimensionless; for other abbreviations please refer to Table I.

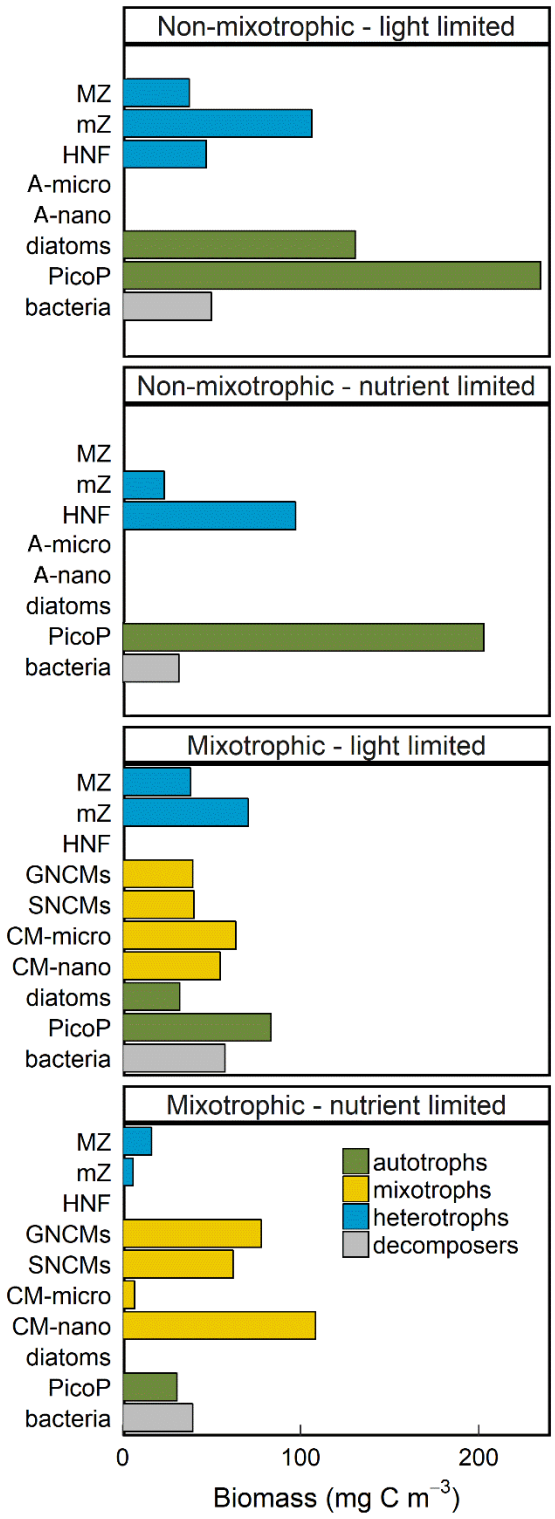

Fig. 3 Community composition for the non-mixotrophic and the mixotrophic food webs in both the light-limited and the nutrient-limited scenarios. Carbon biomass of the different functional groups are given; colours indicate different trophic strategies. Data were averaged for the last year of simulation. MZ – mesozooplankton; A-nano – autotrophic nanoflagellates; A-micro – autotrophic microflagellates; for other abbreviations please refer to Table I.

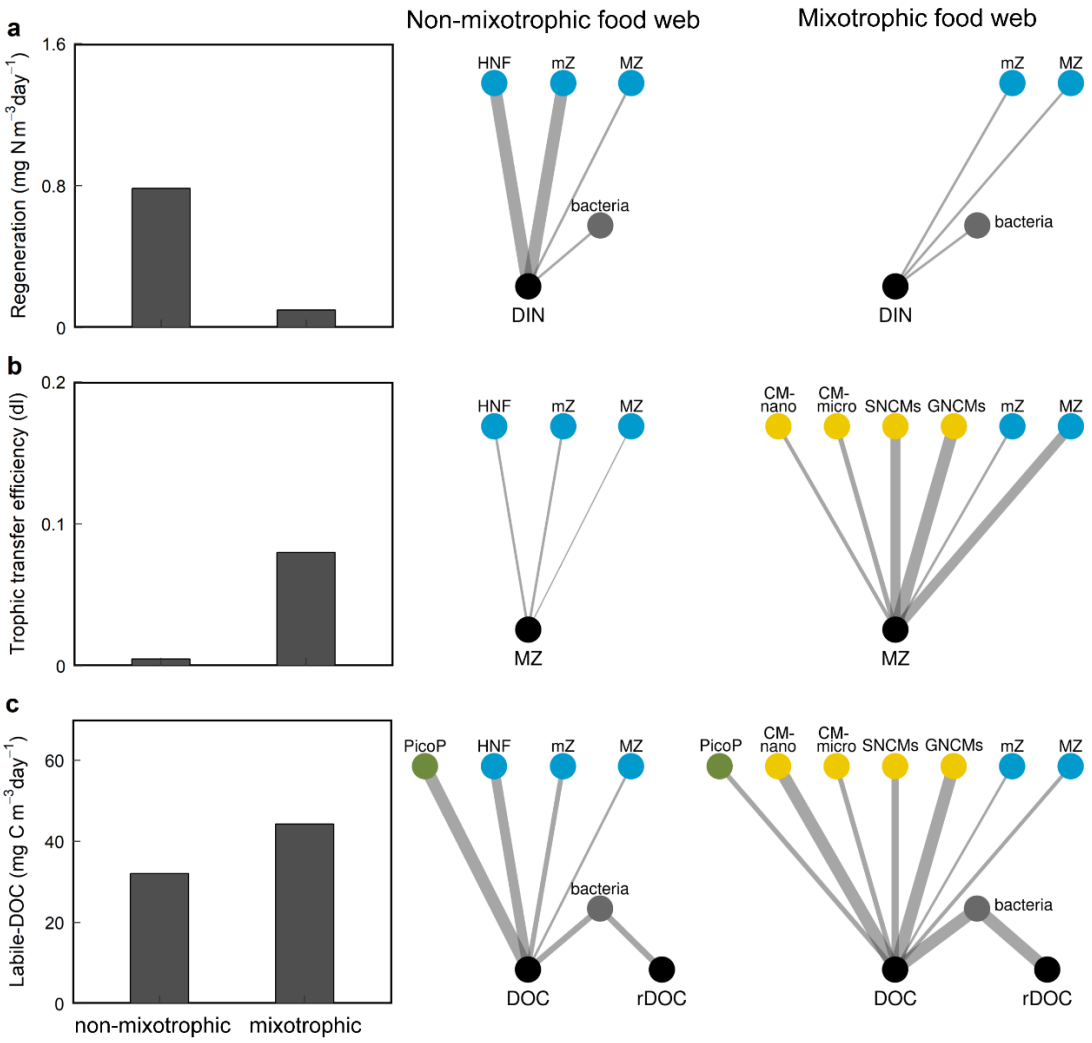

787

788 **Fig. 4** Nutrient limited-scenario for the non-mixotrophic and the mixotrophic food webs. a)
789 ammonium (DIN) regeneration; b) trophic transfer efficiency (measured by the ratio of the total
790 amount of food ingested by mesozooplankton (MZ) by the total gross primary productivity); and c)
791 total production of labile dissolved organic carbon (DOC). Data were averaged for the last year of
792 simulation. Schematics show the relative contribution of functional groups (green–autotrophs,
793 yellow–mixotrophs, blue–heterotrophs, grey–decomposers) to each of the ecosystem properties
794 (black nodes). In panel b, fluxes represent the amount of food ingested by mesozooplankton.
795 rDOC–recalcitrant DOC, dl-dimensionless; for other abbreviations please refer to Table I.

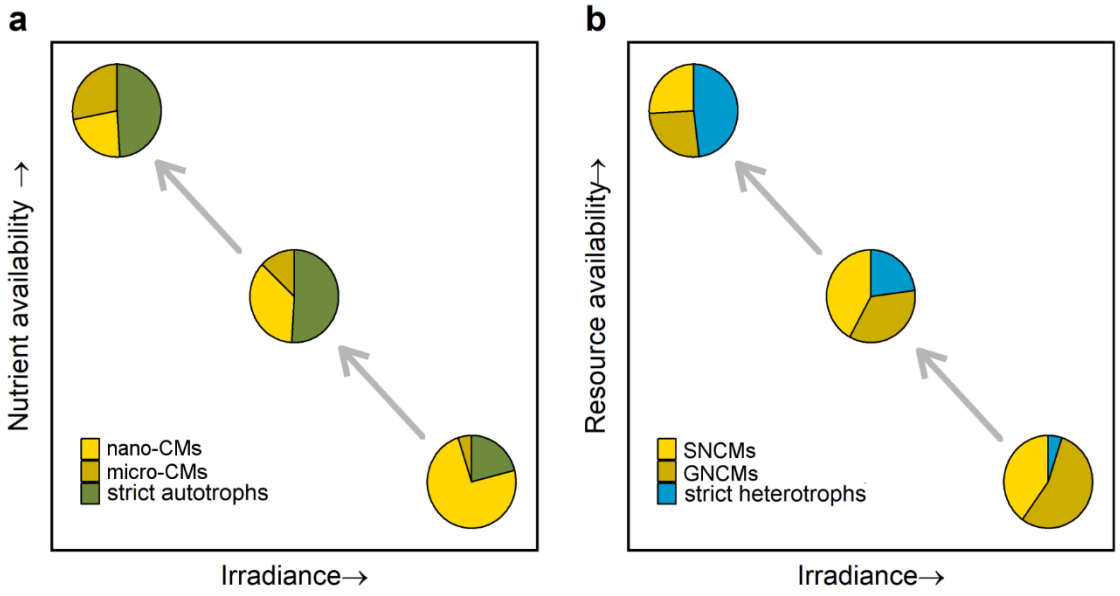

796

797 **Fig. 5** Relative biomass of mixotrophic, strict autotrophic, and strict heterotrophic protists in a
798 gradient from nutrient to light limitation. a) constitutive mixotrophs (CMs) and their strict
799 autotrophic competitors; b) non-constitutive mixotrophs (NCMs) and their strict heterotrophic
800 competitors. Data were averaged for the last year of simulation. Note that area corresponding to
801 high nutrient and high irradiance (upper right corner of the panels) are potentially mutually
802 exclusive due to self-shading; for abbreviations please refer to Table I.

803

804 **Tables**

805 **Table I** Definitions of mixotrophic functional diversity following Mitra *et al*., (2016) and model
806 organisms used in this study

Term	Definition	Model organism
Mixotrophy	The combination of phototrophy and phagotrophy in a single organism	protist plankton
Constitutive mixotrophs (CMs)	Possess their own photosystems; within the model structure these are facultative mixotrophs, i.e. do not need to feed to survive	nanoflagellates (CM-nano) and microflagellates (CM-micro)
Non-constitutive mixotrophs (NCMs)	Need to acquire phototrophic potential from their phototrophic prey and are obligate mixotrophs	specialist (SNCMs) and generalist (GNCMs) forms
Generalist non-constitutive mixotrophs (GNCMs)	NCMs that obtain their phototrophic machinery from diverse phototrophic prey and have poor control over these	oligotrich ciliates
Specialist non-constitutive mixotrophs (SNCMs)	NCMs that obtain their phototrophic machinery from specific phototrophic prey and have high control over these	e.g. *Mesodinium rubrum*
Strict autotrophic competitors	Strictly autotrophic protist plankton; within the model structure these compete with mixotrophs for light and nutrients	Picophytoplankton (PicoP) and diatoms
Strict heterotrophic competitors	Strictly heterotrophic protist plankton; within the model structure these compete with mixotrophs for prey	Heterotrophic nanoflagellates (HNF) and heterotrophic microzooplankton (mZ)

807

808

Table II Results of the Monte-Carlo sensitivity analyses for three targeted model outputs in the mixotrophic food web within the light-limited scenario (sensitivity coefficients of all parameters were statistically significant at $p < 0.001$ and $R^2 > 0.9$). These are ranked (most important first) with respect to their absolute value. Coefficient signs indicate a positive or negative effect on the targeted model outputs, i.e. increase or decrease of the output values, respectively. DOC – dissolved organic carbon and Mesozoo – mesozooplankton; for other abbreviations please refer to Table I and for parameter description refer to Tables S2, S4, and S5

Targeted output	Functional type	Parameter	Coefficient
Ammonium regeneration	PicoP	α_{Chl}	0.34
	CM-nano	NC_{max}	-0.27
	diatoms	α_{Chl}	0.27
	diatoms	$ChlC_{abs}$	0.27
	PicoP	$ChlC_{abs}$	0.24
	CM-micro	NC_{max}	-0.21
	SNCMs	NC_{max}	-0.18
	bacteria	NC_{max}	0.17
Trophic transfer efficiency	CM-nano	S_{opt}	-0.31
	diatoms	α_{Chl}	0.27
	diatoms	$ChlC_{abs}$	0.22
	CM-nano	$ChlC_{abs}$	0.20
	Mesozoo	$Cr_{mesozoo}$	-0.19
	PicoP	$ChlC_{abs}$	-0.19
	Mesozoo	$Cr_{CM\text{-}micro}$	0.17
	CM-nano	α_{Chl}	0.17
Production of labile DOC	diatoms	α_{Chl}	0.50
	diatoms	$ChlC_{abs}$	0.40
	PicoP	α_{Chl}	0.31
	PicoP	$ChlC_{abs}$	0.16
	CM-nano	α_{Chl}	0.15
	CM-nano	$ChlC_{abs}$	0.12
	CM-nano	S_{opt}	0.11
	diatoms	BR	-0.09

α_{Chl}, initial slope of photosynthesis-irradiance curve; BR, basal respiration rate; $ChlC_{abs}$, absolute maximum Chl:C ratio; Cr: slope of capture-prey abundance curve; NC_{max}, maximum N:C ratio; S_{opt}: optimum prey size.

Table III Results of the Monte-Carlo sensitivity analyses for three targeted model outputs in the mixotrophic food web within the nutrient-limited scenario (sensitivity coefficients of all parameters were statistically significant at $p < 0.001$ and $R^2 > 0.9$). These are ranked (most important first) with respect to their absolute value. Coefficient signs indicate a positive or negative effect on the targeted model outputs, i.e. increase or decrease of the output values, respectively. DOC – dissolved organic carbon and Mesozoo – mesozooplankton; for other abbreviations please refer to Table I and for parameter description refer to Tables S2, S4, and S5

Targeted output	Functional type	Parameter	Coefficient
Ammonium regeneration	CM-nano	S_{max}	-0.46
	CM-nano	NC_{max}	-0.20
	bacteria	NC_{max}	0.14
	GNCMs	S_{max}	0.11
	CM-nano	μ_{phot}	0.10
	CM-nano	S_{opt}	-0.10
	SNCMs	S_{max}	0.09
	SNCMs	PC_{max}	0.06
Trophic transfer efficiency	CM-nano	S_{opt}	-0.42
	CM-nano	S_{max}	-0.29
	Mesozoo	Cr_{GNCMs}	0.21
	GNCMs	S_{max}	-0.21
	SNCMs	S_{max}	-0.16
	CM-nano	S_{min}	-0.13
	PicoP	μ_{phot}	-0.12
	bacteria	NC_{max}	0.11
Production of labile DOC	CM-nano	μ_{phot}	0.33
	SNCMs	S_{max}	0.32
	CM-nano	NC_{min}	-0.31
	bacteria	NC_{max}	-0.30
	GNCMs	S_{max}	0.25
	CM-nano	NC_{max}	-0.20
	GNCMs	PC_{max}	0.19
	bacteria	PC_{max}	0.17

Cr: slope of capture-prey abundance curve; NC_{max}, maximum N:C ratio; NC_{min}, minimum N:C ratio; μ_{phot}, maximum phototrophic growth rate; PC_{max}, maximum P:C ratio; S_{max}, maximum prey size; S_{min}, minimum prey size; S_{opt}: optimum prey size.